



ARTICLE

TAK-137, an AMPA-R potentiator with little agonistic effect, has a wide therapeutic window

Akiyoshi Kunugi¹, Maiko Tanaka¹, Atsushi Suzuki¹, Yasukazu Tajima¹, Noriko Suzuki¹, Motohisa Suzuki¹, Shinji Nakamura¹, Haruhiko Kuno², Akihiro Yokota¹, Satoshi Sogabe², Yohei Kosugi³, Yasuyuki Awasaki⁴, Tomohiro Kaku¹ and Haruhide Kimura¹

Activation of α -amino-3-hydroxy-5-methyl-4-isoxazole-propionic acid receptor (AMPA-R) is a promising strategy to treat psychiatric and neurological diseases if issues of bell-shaped response and narrow safety margin against seizure can be overcome. Here, we show that structural interference at Ser743 in AMPA-R is a key to lower the agonistic effect of AMPA-R potentiators containing dihydropyridothiadiazine 2,2-dioxides skeleton. With this structural insight, TAK-137, 9-(4-phenoxyphenyl)-3,4-dihydropyrido[2,1-c][1,2,4]thiadiazine 2,2-dioxide, was discovered as a novel AMPA-R potentiator with a lower agonistic effect than an AMPA-R potentiator LY451646 ((R)-N-(2-(4'-cyanobiphenyl-4-yl)propyl)propane-2-sulfonamide) in rat primary neurons. TAK-137 induced brain-derived neurotrophic factor in neurons in rodents and potently improved cognition in both rats and monkeys. Compared to LY451646, TAK-137 had a wider safety margin against seizure in rats. TAK-137 enhanced neural progenitor proliferation over a broader range of doses in rodents. Thus, TAK-137 is a promising AMPA-R potentiator with potent procognitive effects and lower risks of bell-shaped response and seizure. These data may open the door for the development of AMPA-R potentiators as therapeutic drugs for psychiatric and neurological diseases.

Neuropsychopharmacology (2019) 44:961–970; <https://doi.org/10.1038/s41386-018-0213-7>

INTRODUCTION

The ionotropic glutamate receptor α -amino-3-hydroxy-5-methyl-4-isoxazole-propionic acid (AMPA) receptor (AMPA-R) mediates the vast majority of fast excitatory neurotransmission in the central nervous system [1]. AMPA-Rs are composed of four subunits (GluA1–4), which have flip (i) and flop (o) splice isoforms, and native AMPA-Rs are most likely tetramers generated by the assembly of one or more of these subunits [2–6]. Additional complexity of AMPA-Rs is conferred by RNA editing of a Q/R site in the GluA2 RNA and differential assembly with auxiliary accessory transmembrane proteins such as transmembrane AMPA-R regulatory proteins (TARPs) [7–9]. AMPA-Rs play an important role in synaptic plasticity, which is essential for learning and memory [10]. In fact, AMPA-R potentiators improved cognitive performance in multiple preclinical models [11, 12]. Accumulating evidence suggests that dysfunction of glutamatergic signaling contributes to cognitive deficits such as schizophrenia and Alzheimer's disease. Moreover, AMPA-R activation and consequent brain-derived neurotrophic factor (BDNF) production may have pivotal roles in ketamine's fast antidepressant activity [13]. Thus, activation of AMPA-Rs could be a novel strategy for treating psychiatric and neurological diseases.

AMPA-R agonists, which can activate all AMPA-Rs including resting receptors, have been shown to induce both desensitization of AMPA-R and seizure [14–16]. AMPA-R potentiators are considered to have better pharmacological profiles because of their selective enhancement of physiological activation of AMPA-Rs in the brain. However, AMPA-R potentiators such as LY451646

((R)-N-(2-(4'-cyanobiphenyl-4-yl)propyl)propane-2-sulfonamide), LY451395, and S18986 were reported to demonstrate bell-shaped response in their various pharmacological effects [17–19]. In addition, we observed that LY451646 induced seizure at a 10-fold higher dosage than that required for cognitive improvement in a novel object recognition test in rats. Given the heterogeneity of humans (e.g., metabolic rates, genetics, etc.), these risks would be more serious in clinical trials. Thus, discovery of AMPA-R potentiators with lower risks of bell-shaped response and seizure would be critical for development of AMPA-R potentiators as therapeutic drugs.

To discover AMPA-R potentiators with lower risks of bell-shaped response and seizure, we explored in vitro assays that can detect the bell-shaped dose responses. We found that LY451646 and LY451395 started to exhibit a bell-shaped response at concentrations at which they started to show agonistic effect in BDNF protein production in primary neurons [20]. Surprisingly, LY451646 and LY451395 showed potent agonistic effects in a Ca^{2+} influx assay with primary neurons, but not with a cell line expressing AMPA-Rs. Moreover, a novel AMPA-R potentiator, HBT1, with low agonistic effect in the Ca^{2+} influx assay with primary neurons, had lower risk of bell-shaped response in in vitro BDNF production compared with LY451395 [20]. HBT1 and LY451395 bound to a pocket in the ligand-binding domain (LBD) of AMPA-R with different binding modes. Thus, optimization of HBT1-site binders by giving careful consideration to the relationship between binding mode and functional outcome may be important for discovering potent and safer AMPA-R potentiators.

¹Neuroscience Drug Discovery Unit, Research, Takeda Pharmaceutical Company Limited, Fujisawa, Japan; ²Bio-Molecular Research Laboratories, Research, Takeda Pharmaceutical Company Limited, Fujisawa, Japan; ³Drug Metabolism and Pharmacokinetics Research Laboratories, Research, Takeda Pharmaceutical Company Limited, Fujisawa, Japan and ⁴Drug Safety Research and Evaluation, Research, Takeda Pharmaceutical Company Limited, Fujisawa, Japan
Correspondence: Haruhide Kimura (haruhide.kimura@takeda.com)

Received: 2 April 2018 Revised: 27 August 2018 Accepted: 3 September 2018
Published online: 12 September 2018

Here, we report the discovery of TAK-137, 9-(4-phenoxyphenyl)-3,4-dihydropyrido[2,1-c][1,2,4]thiadiazine 2,2-dioxide, as a novel AMPA-R potentiator with lower agonistic effects based on the characterization of the relationship between binding mode at the HBT1-site and functional outcome of dihydropyridothiadiazine 2,2-dioxides. TAK-137 induced BDNF production in rat primary neurons and mouse hippocampus, showed potent cognitive improvement in both rats and monkeys, and had lower risks of bell-shaped responses and seizures in rats. These data may open the door for the development of AMPA-R potentiators as therapeutic drugs for psychiatric and neurological diseases.

MATERIALS AND METHODS

Chemicals

HBT1, TAK-137, Compound-1 (9-(4-isopropoxyphenyl)-3,4-dihydropyrido[2,1-c][1,2,4]thiadiazine 2,2-dioxide), Compound-2 (9-(4-*tert*-butylphenyl)-3,4-dihydropyrido[2,1-c][1,2,4]thiadiazine 2,2-dioxide), and LY451646 were synthesized by Takeda Pharmaceutical Company Limited. Additional information is described in the Supplementary Information.

Ca^{2+} influx assay using cell lines expressing AMPA-Rs or GluK1/2 receptors

Ca^{2+} influx assays using cell lines expressing AMPA-Rs or GluK1/2 receptors were performed as described elsewhere [20], with some modifications. Details are described in the Supplementary Information.

Ca^{2+} influx assay using primary neurons

Ca^{2+} influx assay using primary neurons was performed as described elsewhere [20].

Whole-cell patch-clamp recording using primary neurons

Whole-cell patch-clamp recording using primary neurons was performed as described elsewhere [20].

BDNF production in primary neurons

BDNF production in primary neurons was measured as described elsewhere [20].

Scintillation proximity assay

The scintillation proximity assays (SPAs) were performed as described elsewhere [20], with some modifications. Details are described in the Supplementary Information.

Binding assay using rat hippocampal membranes or cell membranes prepared from cell lines expressing GluA1i

The binding assays were performed as described elsewhere [20], with some modifications. Details are described in the Supplementary Information.

X-ray crystallography of the GluA2o LBD/compound complex

Methods are described in the Supplementary Information.

Animals

Mice (ICR and C57BL/6J) and rats (Sprague–Dawley (IGS) and Long–Evans) were housed in groups of 2–5/cage in a light-controlled room (12 h light/dark cycle) with free access to food and water and were habituated to the cages for more than 1 week prior to experiments. The monkeys were housed individually in a light-controlled room (12 h light/dark cycle). They were fed once daily, and water was available *ad libitum*. The care and use of the animals and the experimental protocols used in this research were approved by the Experimental Animal Care and Use Committee of Takeda Pharmaceutical Company Limited.

Drug administration

TAK-137 and LY451646 suspended in 0.5% (w/v) methylcellulose in distilled water were administered orally (p.o.) to individual animals. For delayed matching-to-sample (DMTS) tasks, LY451646 was dissolved in 10% cremophor (w/v) in sterile distilled water and was administered subcutaneously (s.c.).

Proliferation of neural progenitor cells in the hippocampus

Number of 5-bromo-2'-deoxyuridine (BrdU)-positive nuclei was quantified using flow cytometry as previously described, with some modifications [21]. Details are described in the Supplementary Information.

Novel object recognition test

Novel object recognition tests (NORTs) were performed as previously described [22], with modified administration timing of compounds. Details are described in the Supplementary Information.

DMTS tasks

DMTS tasks were performed using a Cambridge Neuropsychological Test Automated Battery system. Details are described in the Supplementary Information.

Evaluation of seizure

Methods of evaluation of seizure induction are described in the Supplementary Information.

Statistics

Statistical methods are described briefly in the figure legends. Details are described in the Supplementary Information.

RESULTS

Compound-1 had lower agonistic effect than Compound-2 in primary neurons

To discover novel AMPA-R potentiators with lower agonistic effects, we screened a chemical library by the SPA using [^3H]-HBT1 and a His-tagged GluA2o LBD protein (His-LBD), and identified a novel chemotype (dihydropyridothiadiazine 2,2-dioxides). Two dihydropyridothiadiazine 2,2-dioxide derivatives, Compound-1 and Compound-2 (Fig. 1a), inhibited binding between [^3H]-HBT1 and LBD with an inhibition constant (K_i) of 0.082 and 0.019 μM , respectively, in the SPA (Fig. 1b). Compound-1 and Compound-2 also inhibited binding between [^3H]-HBT1 and naive rat AMPA-R, with K_i of 0.018 and 0.006 μM , respectively, in a binding assay with hippocampal membranes (Fig. 1c). Compound-1 and Compound-2 may have similar binding affinity to the LBD of AMPA-R. Compound-1 and Compound-2 induced Ca^{2+} influx in a glutamate-dependent manner in Chinese hamster ovary (CHO) cells expressing GluA1i and TARP γ -2 (GluA1i CHO cells) (Fig. 1d): a log median effective concentration (LogEC_{50}) was -5.98 ± 0.023 and -6.20 ± 0.003 M, respectively. Agonistic effects of AMPA-R potentiators in Ca^{2+} influx assay were observed in primary neurons, but not in a cell line expressing AMPA-Rs [20]. Thus, we evaluated Compound-1 and Compound-2 in Ca^{2+} influx assay using primary neurons to measure their LogEC_{50} and maximum effect (Emax): LogEC_{50} (Emax) of Compound-1 in the presence and absence of AMPA was -6.33 ± 0.037 (128%) and -5.30 ± 0.234 (14%) M, respectively, while that of Compound-2 in the presence and absence of AMPA was -6.82 ± 0.071 (163%) and -5.79 ± 0.132 (90%) M, respectively (Fig. 1e). Compound-1 may have lower agonistic effect than Compound-2 in primary neurons. Compound-2 (and Compound-1) did not inhibit [^3H]-AMPA binding to hippocampus membranes (Fig. 1f). Agonistic effect of Compound-2 may not be associated with its binding to agonist site.

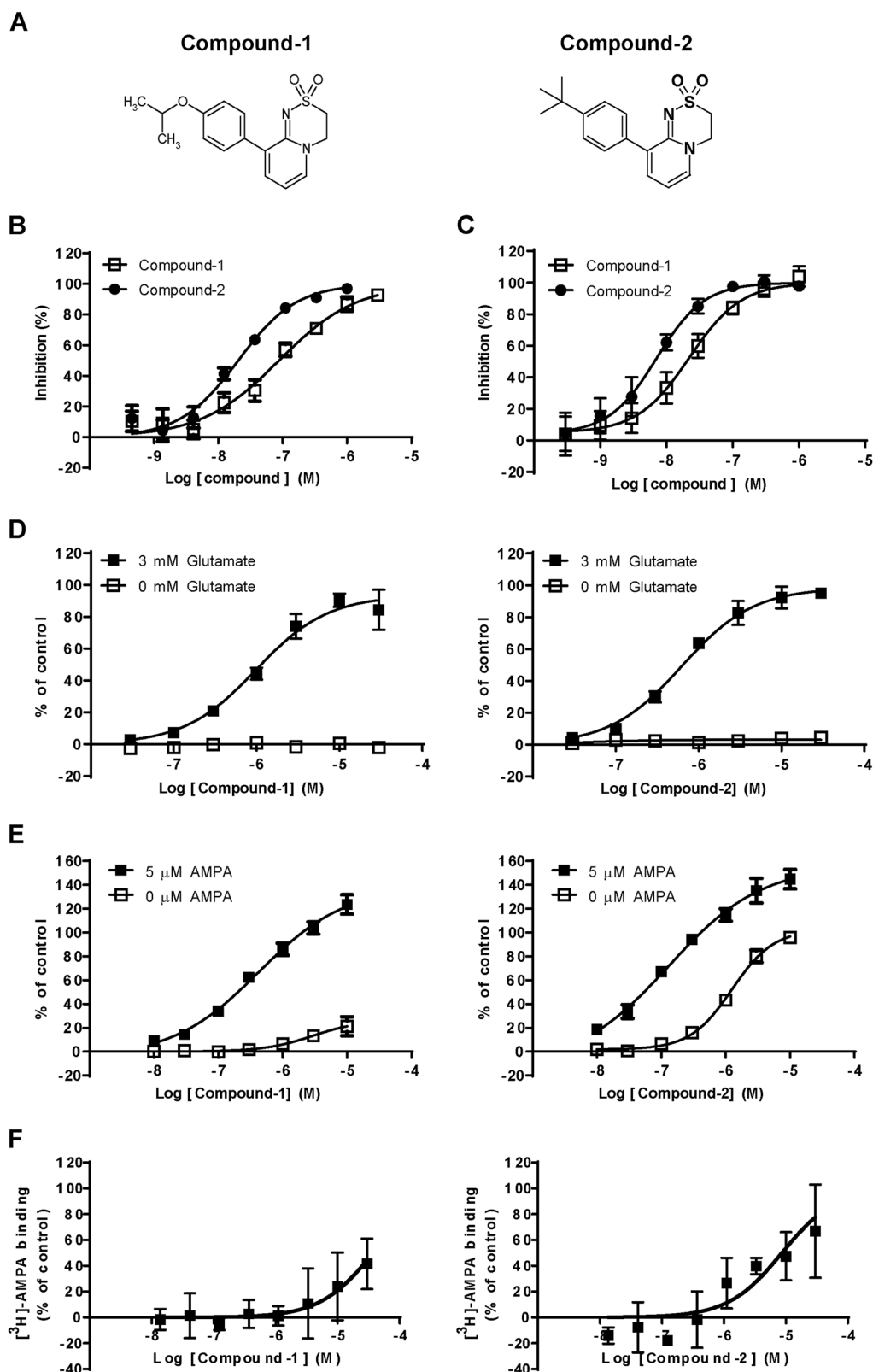


Fig. 1 Compound-1 had lower agonistic effect than Compound-2 in primary neurons. **a** Chemical structures of Compound-1 and Compound-2. **b** Displacement studies with Compound-1 and Compound-2 by SPA using $[^3\text{H}]\text{-HBT1}$ and His-LBD. **c** Displacement studies with Compound-1 and Compound-2 by binding assay using $[^3\text{H}]\text{-HBT1}$ and hippocampal membranes. Data (**b**, **c**) are presented as the mean \pm SD ($n = 3\text{--}4$). **d** Effects of Compound-1 and Compound-2 on Ca^{2+} influx in primary neurons in the presence or absence of 3 mM glutamate. **e** Effects of Compound-1 and Compound-2 on Ca^{2+} influx in primary neurons in the presence or absence of 5 μM AMPA. The experiments were repeated at least twice, and representative graphs (**d**, **e**) are shown. Data are presented as mean \pm SD ($n = 3$). **f** Effects of Compound-1 and Compound-2 on $[^3\text{H}]\text{-AMPA}$ binding to rat hippocampal membranes. Data are presented as mean \pm SD ($n = 3$)

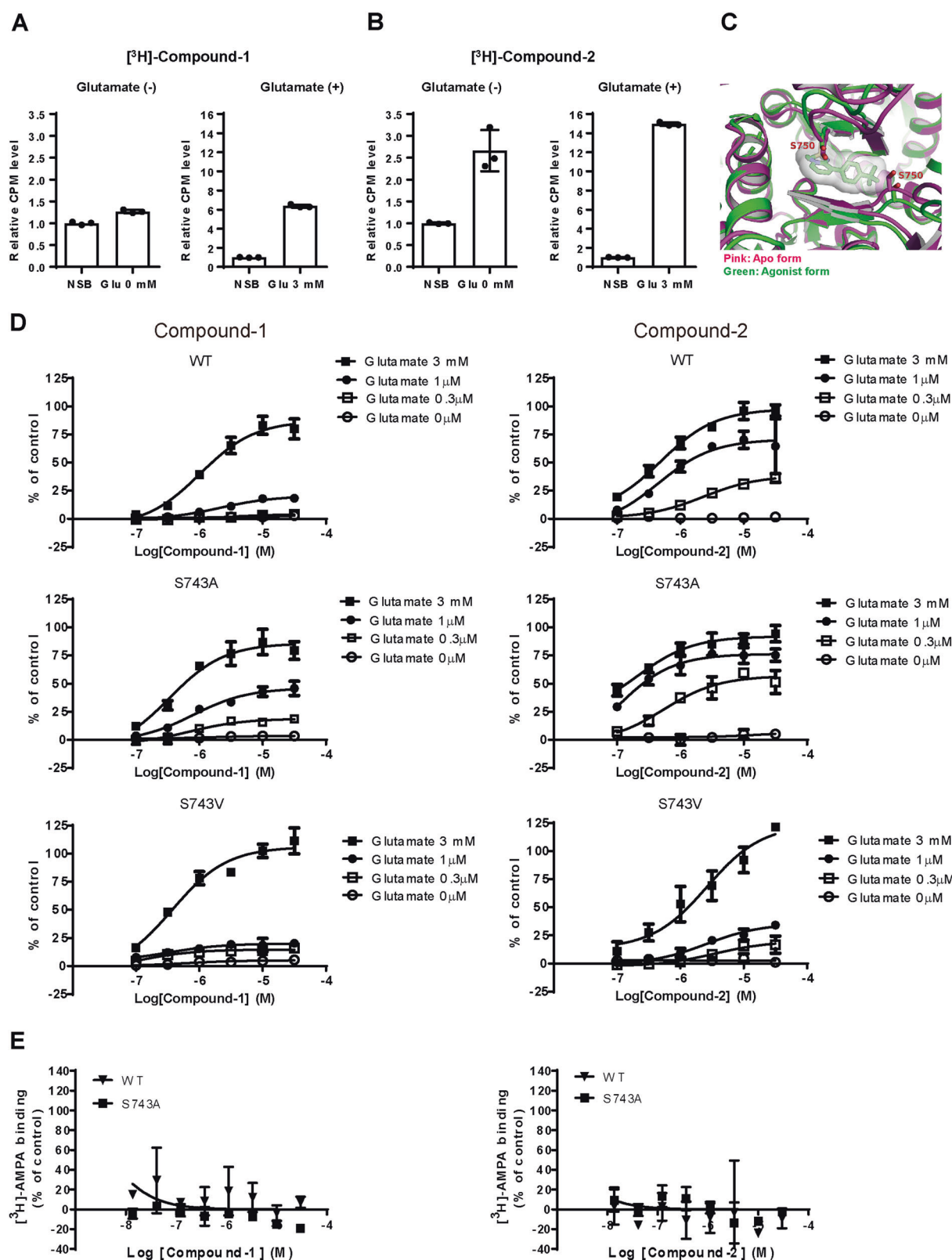


Fig. 2 Compound-1, but not Compound-2, bound to AMPA-R in a glutamate-dependent manner by the steric interference at Ser743. **a, b** Binding of [³H]-Compound-1 (**a**) or [³H]-Compound-2 (**b**) to hippocampal membranes in the presence or absence of 3 mM glutamate. Non-specific binding (NSB) was determined with 10 μM NBQX. Data (**a, b**) are presented as mean ± SD (*n* = 3). **c** Superposition of LBDs of full-length GluA2 from the agonist form (PDB code 4U1W) and the apo form (PDB code 4U2P). Compound-2 is also superposed for reference. **d** Effects of Compound-1 and Compound-2 on Ca²⁺ influx in CHO cells expressing GluA1i WT, GluA1i S743A, and GluA1i S743V in the presence or absence of glutamate (0.3 μM, 1 μM, and 3 mM). S743 in GluA1i LBD corresponds to S750 in GluA2o LBD. Data are presented as mean ± SD (*n* = 3). **e** Effects of Compound-1 and Compound-2 on [³H]-AMPA binding to GluA1i WT or GluA1i S743A. Data are presented as mean ± SD (*n* = 3)

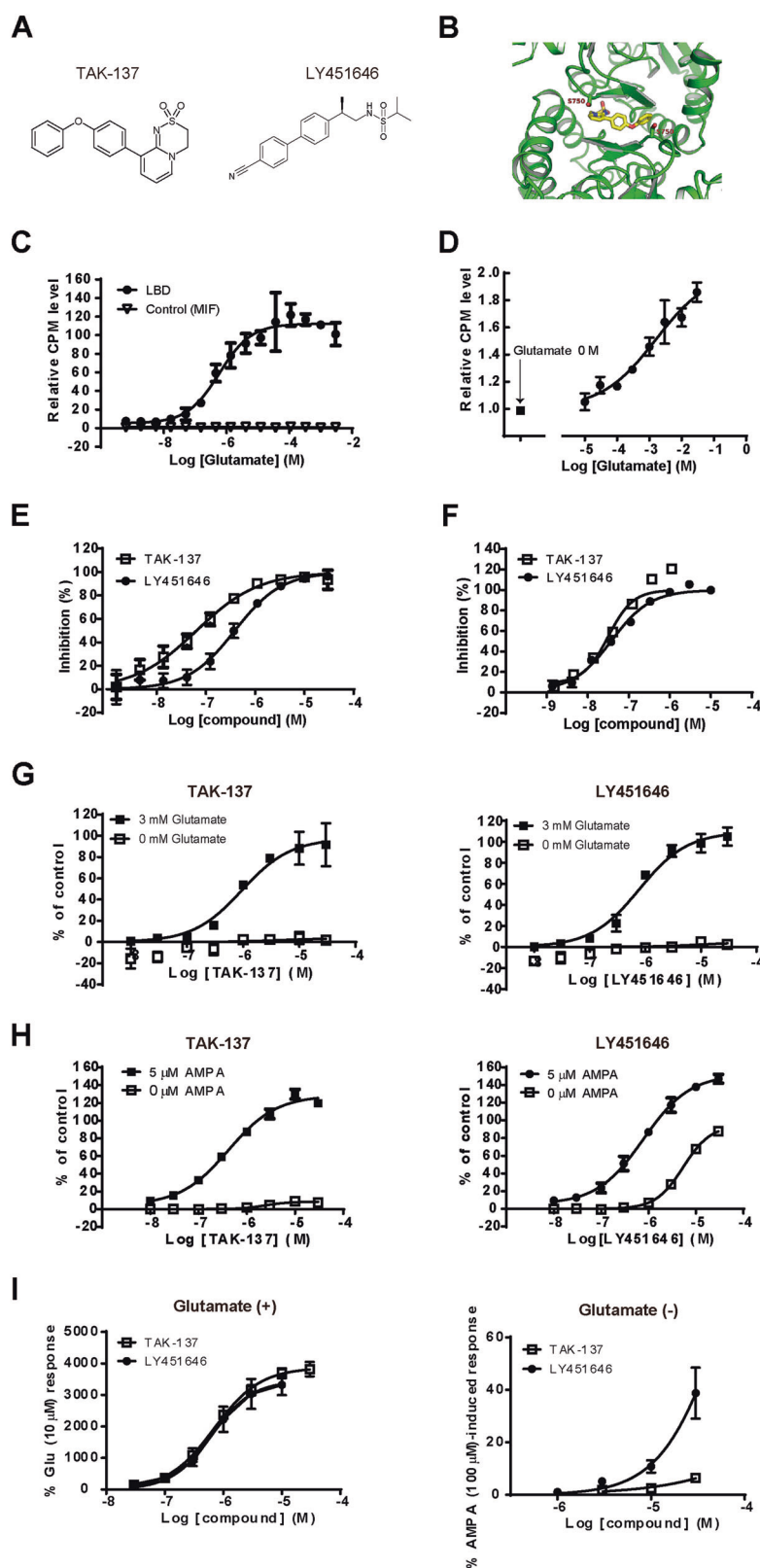
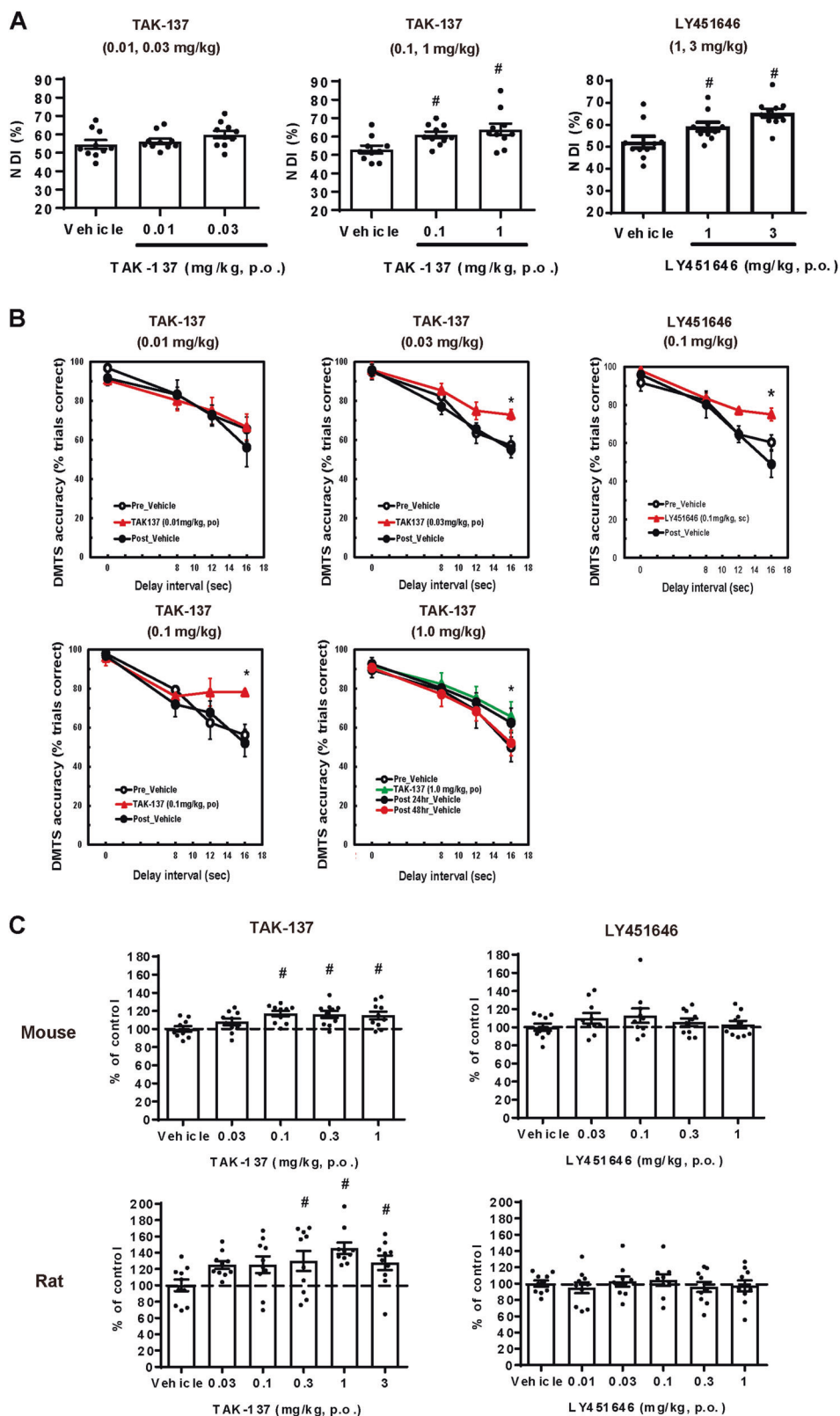


Fig. 3 TAK-137 had lower agonistic effects than LY451646. **a** Chemical structure of TAK-137 and LY451646. **b** Crystal structure of GluA2o LBD in complex with TAK-137. **c, d** Effects of glutamate on the binding of [³H]-TAK-137 to His-LBD (**c**) and hippocampal membranes (**d**). Data are presented as mean \pm SD ($n = 3$). **e, f** Displacement studies with TAK-137 and LY451646 by SPA using [³H]-HBT1 and His-LBD and binding assay using [³H]-HBT1 and hippocampal membranes. Data are presented as the mean \pm SD ($n = 3-4$). **g, h** Effects of TAK-137 and LY451646 on Ca²⁺ influx in GluA1i CHO cells (**g**) and primary neurons (**h**) in the presence or absence of agonist. The experiments were repeated at least twice, and representative graphs are shown. Data are presented as mean \pm SD ($n = 3$). **i** Effects of TAK-137 and LY451646 on AMPA receptor-mediated currents in the presence or absence of 10 μ M glutamate in electrophysiological study using primary neurons. Data are presented as mean \pm SEM ($n = 4-9$)



Compound-1, but not Compound-2, bound to AMPA-R in a glutamate-dependent manner by using the steric interference at Ser743

To understand the mechanism of action underlying the different agonistic effects of Compound-1 and Compound-2, we examined

binding modes of these compounds. [3 H]-Compound-1 bound to hippocampal membranes in the presence of 3 mM glutamate, but not in the absence of glutamate (Fig. 2a). On the other hand, [3 H]-Compound-2 bound to hippocampal membranes both in the presence and absence of glutamate (Fig. 2b).

Fig. 4 TAK-137 produced potent cognitive improvement in rats and monkeys and induced proliferation of rodent hippocampal neural progenitor cells over a broader range of doses compared to LY451646. **a** Cognitive-enhancing effects of TAK-137 and LY451646 on rat NORT. Data are presented as the mean \pm SEM ($n = 10$). Significant difference from vehicle-treated group was analyzed using the one-tailed Williams' test (TAK-137: $^*P \leq 0.025$, d.f. = 27, $t = 2.3$ (0.1 mg/kg), 3.2 (1 mg/kg), LY451646: $^*P \leq 0.025$, d.f. = 27, $t = 2.2$ (1 mg/kg), 4.2 (3 mg/kg)). **b** Cognitive-enhancing effects of TAK-137 and LY451646 on monkey DMTS task. Data are presented as the mean \pm SEM ($n = 4$). Significant difference from vehicle-treated group was analyzed using two-way ANOVA (TAK-137: $^*P \leq 0.05$, $F_{1,6} = 4.0$ (0.03 mg/kg), $F_{1,6} = 6.7$ (0.1 mg/kg), $F_{1,6} = 6.1$ (1 mg/kg), LY451646: $^*P \leq 0.05$, $F_{1,6} = 7.2$ (0.1 mg/kg)). **c** Effects of TAK-137 and LY451646 on the number of BrdU-positive cells in mouse or rat hippocampus. TAK-137 or LY451646 was orally administered to mice or rats for 4 days and tissues were isolated the next day. Data are presented as the mean \pm SEM ($n = 9$ –10). Significant difference from vehicle-treated group was analyzed using the one-tailed Williams' test (mouse: $^*P \leq 0.025$, d.f. = 45, $t = 3.3$ (0.1 mg/kg), 3.2 (0.3 mg/kg), 3.1 (1 mg/kg), rat: $^*P \leq 0.025$, d.f. = 54, $t = 2.4$ (0.3 mg/kg), 3.7 (1 mg/kg), 3.0 (3 mg/kg))

We next investigated the interactions of Compound-1 and Compound-2 with the LBD by X-ray crystallographic analysis. The LBD is highly conserved among GluA1–4 subunits, with approximately 80% sequence identity. The structures of the LBD of GluA2–4 have been reported to be almost identical except for the flip and flop splice forms [23]. Compound-1 and Compound-2 exhibited little subunit selectivity (Table S1); thus, we employed the well-characterized GluA2o LBD in this structural analysis by X-ray crystallography. Both compounds bound to the cleft composed of the dimer interface between two protomers (Fig. S1A, S1B). The structure of the agonist/Compound-2-bound LBD in the channel-open state was compared with that of the antagonist/Compound-2-bound LBD in the channel-closed state as an example of the agonist-free form. No clear structural differences were observed in the vicinity of the AMPA-R potentiator-binding site, although known structural rearrangement of the S1S2 clam shell was observed (Fig. S1C). However, structural comparison of the full-length GluA2o between the channel-open state and the channel-closed state revealed that main-chain atoms around Ser750 into the potentiator-binding cleft are shifted by the agonist binding (Fig. 2c). Furthermore, the terminal substituent of Compound-2 (*tert*-butyl group), which is different from that of Compound-1 (the isopropoxy group), was located in the vicinity of the serine residue (Fig. 2c). From these data, we speculated that Ser750 may prevent Compound-1, but not Compound-2, from binding in the “apo” agonist-free state due to steric interference.

Ser750 in GluA2o corresponds to Ser743 in GluA1i; thus, we introduced a mutation at Ser743 (S743A or S743V) in GluA1i to modify the possible steric interference between Compound-1 or Compound-2 and AMPA-R. Theoretically, S743A lowers this steric interference, while S743V increases it. Interestingly, S743A increased the maximum response of Compound-1 at lower concentrations (0.3 and 1 μ M) of glutamate, but not at high concentration (3 mM) of glutamate, in the Ca^{2+} influx assays using GluA1i-transfected CHO cells (Fig. 2d, middle left panel). On the other hand, S743A barely affected the maximum response of Compound-2 at all tested concentrations of glutamate (Fig. 2d, middle right panels). Compound-1 and Compound-2 did not activate S743A GluA1i in the absence of glutamate (Fig. 2d, middle panels). In S743V GluA1i, Compound-2, which can activate wild-type (WT) GluA1i at lower concentrations (0.3 and 1 μ M) of glutamate compared to Compound-1 (Fig. 2d, upper right panel), lost its higher sensitivity to glutamate for GluA1i activation (Fig. 2d, lower right panel). S743V did not affect the sensitivity of Compound-1 to glutamate for GluA1i activation (Fig. 2d, lower left panel). If S743A modulates the cooperativity between the compounds and the agonist, the concentration of glutamate required for GluA1i activation by each compound would be affected. S743A did not affect the impact of Compound-1 or Compound-2 on the binding between [^3H]-AMPA and GluA1i (Fig. 2e). Therefore, S743A may not affect the cooperativity between the compounds and the agonist in GluA1i CHO.

TAK-137 had lower agonistic effects than LY451646

We designed dihydropyridothiadiazine 2,2-dioxides with minimum binding affinity to the LBD in the channel-closed state by the steric interference at Ser743 in GluA1i (Ser750 in GluA2o), and finally discovered TAK-137 as a drug candidate (Fig. 3a). TAK-137 bound to the cleft composed of the dimer interface between two protomers: a bulky phenoxy group of TAK-137 was located in the vicinity of Ser750 (Fig. 3b and Fig. S2). [^3H]TAK-137 bound to the His-LBD and hippocampal membranes in a glutamate-dependent manner (Figs. 3c, d). LY451646 (Fig. 3a) also binds to the LBD of AMPA-R [24, 25]. As expected, TAK-137 and LY451646 inhibited binding between [^3H]-HBT1 and LBD with K_i of 0.061 and 0.363 μ M, respectively, and inhibited binding between [^3H]-HBT1 and hippocampal membranes with K_i of 0.025 and 0.031 μ M, respectively (Figs. 3e, f). TAK-137 and LY451646 induced Ca^{2+} influx in an agonist-dependent manner in GluA1i CHO cells (Fig. 3g): LogEC_{50} was -5.98 ± 0.021 and -6.10 ± 0.014 M, respectively. Similar to Compound-1, S743A lowered the concentration of glutamate required to activate GluA1i by TAK-137 in Ca^{2+} influx assay (Fig. S3). LY451646 showed potent agonistic effect in BDNF production in primary neurons [20]; thus, we compared agonistic effects of TAK-137 and LY451646 in primary neurons. TAK-137 induced Ca^{2+} influx in an agonist-dependent manner in primary neurons, while LY451646 induced Ca^{2+} influx both in the presence and absence of AMPA (Fig. 3h): LogEC_{50} (Emax) of TAK-137 in the presence and absence of AMPA was -6.36 ± 0.020 (126%) and -5.64 ± 0.019 (10%) M, respectively, and that of LY451646 was -6.30 ± 0.193 (148%) and -5.23 ± 0.033 (86%) M, respectively. OXP1, an AMPA-R potentiator, showed little agonistic effect in the Ca^{2+} influx assay using primary neurons, while it elicited remarkable agonistic effect in the patch-clamp study using primary neurons [20]. Thus, we also evaluated TAK-137 and LY451646 in the patch-clamp study. TAK-137 induced AMPA-R-mediated current only in the presence of glutamate in electrophysiological study using primary neurons, while LY451646 induced AMPA-R-mediated currents both in the presence and absence of glutamate (Fig. 3i). Thus, TAK-137 may have a lower agonistic effect than LY451646. Similar to Compound-1, TAK-137 did not inhibit [^3H]-AMPA binding to naive AMPA-R or GluA1i (Fig. S4).

The slow recovery from potentiation may cause sustained activation of AMPA-R and induce seizures; however, AMPA-R activation induced by TAK-137 or LY451646 showed similar recovery duration (90 s) from potentiation in an electrophysiological study using primary neurons (Fig. S5). Subunit selectivity of AMPA-R potentiators might also affect their functional outcomes [26]; however, both TAK-137 and LY451646 showed little subunit selectivity (Table S1). Therefore, the profiles of TAK-137 and LY451646, excluding agonistic activity, looked very similar. TAK-137 at 10 μ M had no significant activity against 98 targets except vasopressin V2 receptors at Ricerca Biosciences (Concord, OH, USA) (Table S2).

Table 1. Rates of seizure in rats and monkeys after acute treatment of compounds

| | | 10 mg/kg | 100 mg/kg | 1000 mg/kg | 100 mg/kg (Nanocrystal) |
|----------|--------|----------------|-----------|------------|-------------------------|
| TAK-137 | Rat | 0% | 0% | 0% | 33% |
| | Monkey | 0% | 0% | – | – |
| | | 1 mg/kg | 3 mg/kg | 10 mg/kg | 30 mg/kg |
| LY451646 | Rat | – | 0% | 33% | 100% |
| | Monkey | – ^a | – | – | – |

Rats ($n = 3$) and monkeys ($n = 4$) were administered TAK-137 and observed for up to 8 h after the administration. Rats ($n = 3$) were administered LY451646 and observed for up to 4 h after the administration

^a Acute treatment of LY451646 at 1 mg/kg, s.c. induced vomiting in monkeys

TAK-137 produced potent cognitive improvement with a wider safety margin against seizure in rats and monkeys and induced proliferation of rodent hippocampal neural progenitor cells over a broader range of doses compared to LY451646

We examined the effect of TAK-137 and LY451646 on cognitive function in rats and monkeys. TAK-137 at 0.1 and 1 mg/kg, p.o., but not 0.01 and 0.03 mg/kg, p.o., significantly increased novelty discrimination index (NDI) in rat NORT, while LY451646 at 1 and 3 mg/kg, p.o., but not at 0.3 mg/kg, p.o., significantly increased NDI (Fig. 4a and Fig. S6). TAK-137 at 0.03, 0.1, and 1 mg/kg, p.o., but not 0.01 mg/kg, p.o., significantly increased DMTS accuracy in monkey DMTS task, while LY451646 at 0.1 mg/kg, s.c., but not at 0.03 mg/kg, s.c., significantly increased DMTS accuracy (Fig. 4b and Fig. S7). TAK-137 may have a lower risk of bell-shaped dose response in cognitive improvement in monkeys. Note that monkeys used in the study at 0.01 and 1 mg/kg were different from those used at the other dose levels; therefore, a direct comparison of robustness could not be performed.

We next examined the effect of TAK-137 and LY451646 on seizure in rats and monkeys. Acute treatment of TAK-137 did not induce seizures at up to 1000 mg/kg, p.o. in rats. Nanocrystal formulation of TAK-137 at 100 mg/kg, p.o., which produced a higher plasma concentration than conventional formulation of TAK-137 at 1000 mg/kg, p.o., induced seizures in rats (Table 1). Acute treatment of LY451646 at 10 and 30 mg/kg, p.o. induced seizure in rats (Table 1). Acute treatment of TAK-137 did not induce seizures at up to 100 mg/kg, p.o. in monkeys (Table 1). Acute treatment of LY451646 at 1 mg/kg, s.c. in monkeys induced vomiting. Thus, we did not administer LY451646 at doses higher than 1 mg/kg, s.c. in monkeys. Based on these results, we calculated the exposure margins of TAK-137 and LY451646 between cognitive improvement and the absence of seizures in rats. For this calculation, the area under the brain drug concentration–time curve (AUC_{brain}) values and brain C_{max} values of compounds in rats (Tables S3 and S4) were used. TAK-137 had a 116-fold (AUC_{brain}) or a 43.7-fold (brain C_{max}) exposure margin in rats, while LY451646 had a 3.1-fold (AUC_{brain}) and a 7.5-fold (brain C_{max}) exposure margin. For a safety margin of TAK-137 in monkeys, we performed the calculation using AUC_{plasma} and plasma C_{max} values (Table S5). TAK-137 had at least a 49-fold (AUC_{plasma}) or a 48-fold (plasma C_{max}) exposure margin in monkeys.

If the wider safety margin of TAK-137 was based on its agonist-dependent activation of AMPA-R, more robust activation of AMPA-R by TAK-137 would be expected by increasing the agonist levels. AMPA-R activation by TAK-137 increased BDNF production in rat primary neurons (Fig. S8A). Intravenous (i.v.) administration of AMPA dose-dependently increased BDNF messenger RNA (mRNA) levels in the mouse hippocampus (Fig. S8B). Therefore, BDNF mRNA level in hippocampus could be a good in vivo pharmacodynamic (PD) marker for AMPA-R activation. We assessed BDNF production by TAK-137 by co-injecting a low dose of AMPA. TAK-137 at 3 and 10 mg/kg, p.o. dose-dependently increased in BDNF

mRNA levels in the hippocampus of AMPA (3.5 mg/kg, i.v.)-treated mice (Fig. S8C). TAK-137 alone did not increase BDNF levels under these experimental conditions (Fig. S8D). TAK-137-free fraction available for AMPA-R activation dose-dependently may increase even at higher dosage than 1 mg/kg in the mouse hippocampus.

LY451646 was reported to enhance proliferation of neural progenitor cells in rat hippocampus with a bell-shaped response. To examine whether TAK-137 shows efficacy over a broader range of doses than LY451646, we investigated the effect of TAK-137 and LY451646 on proliferation of progenitor cells. TAK-137 significantly increased the number of BrdU-positive cells at 0.1–1 mg/kg, p.o. (mouse) and at 0.3–3 mg/kg, p.o. (rat), while LY451646 did not significantly increase the number of BrdU-positive cells under our experimental conditions at doses up to 1 mg/kg, p.o. (Fig. 4c). Therefore, TAK-137 may increase proliferation of progenitor cells in hippocampus over a broader range of doses. However, it remains open whether TAK-137 would demonstrate a broader effective-dose range than LY451646 in an assay in which LY451646 shows a bell-shaped response.

Down-regulation of AMPA-R following chronic stimulation by TAK-137 is also a concern. To investigate receptor desensitization, AMPA-R activation-dependent BDNF mRNA production was assessed in mice after repeated treatment with TAK-137 at 0.1 mg/kg, p.o.: TAK-137 at ≥ 0.1 mg/kg, p.o. increased the proliferation of progenitor cells and produced cognitive improvement in rats (Fig. 4a, c). AMPA-induced BDNF mRNA expression did not change after 14 days of treatment with TAK-137 at 0.1 mg/kg, p.o. (Fig. S9). TAK-137 may have a low risk of receptor desensitization by repetitive dosing.

DISCUSSION

As HBT1-site binders, we identified two dihydropyridothiadiazine 2,2-dioxide derivatives, Compound-1 and Compound-2; Compound-1 had a lower agonistic effect than Compound-2. Binding assay and X-ray crystallography analysis revealed that Compound-1, but not Compound-2, would bind to the LBD in a glutamate-dependent manner (Fig. 2a) due to the steric interference at Ser750 in GluA2o (Fig. 2c), which corresponds to Ser743 in GluA1i. S743A, which lowers this possible steric interference, increased Compound-1's sensitivity to glutamate in the GluA1i activation, while S743V, which increases this possible steric interference, increased the concentration of glutamate required to activate GluA1i by Compound-2 in Ca^{2+} influx assay (Fig. 2d). It is not known whether the conformation of this AMPA-R potentiator-binding site changes by interaction with low concentrations of glutamate. The results of the mutant studies support the idea of glutamate-dependent continuous structural change. Design and discovery of dihydropyridothiadiazine 2,2-dioxides with no or little binding affinity to the LBD in the channel-closed state may lead to the discovery of AMPA-R potentiators with lower agonistic effect. Note that the steric interference at Ser743 could not explain the low agonistic profile of HBT1, which does not have

dihydropyridothiadiazine 2,2-dioxide skeleton [20]. Thus, an original approach for lowering agonistic effect should be established for each chemotype.

Ki values of the compounds, especially LY451646, in the SPA and the binding assay using hippocampal membranes were different. Importantly, native AMPA-Rs are most likely tetramers generated by the assembly of eight subunits, and auxiliary accessory transmembrane proteins such as TARPs are known to affect this assembly. Thus, it would be difficult to accurately reconstruct the structure of naive AMPA-R by purified recombinant LBD of AMPA-R. The structural differences in the AMPA-R used in these assays may be associated with the different Ki values of compounds measured by these two assays, although further studies are needed.

Based on the hypothesis to lower agonistic activity through the steric interference at Ser743, we identified TAK-137 with a lower agonistic effect than LY451646. TAK-137 had a wider safety margin against seizure (116-fold (AUC_{brain}), 43.7-fold (brain C_{max})) than LY451646 (3.1-fold (AUC_{brain}), 7.5-fold (brain C_{max})) in rats. Furthermore, TAK-137 showed a wide safety margin against seizure (>49-fold (AUC_{plasma}), >48-fold (plasma C_{max})) in monkeys. After co-administration of the agonist, AMPA, TAK-137 at doses of 3 and 10 mg/kg produced a greater increase in BDNF production, suggesting that the concentration of free TAK-137 available for receptor binding was increased under these conditions. However, due to limitations in the amount of glutamate (endogenous agonist), free TAK-137 at higher doses may be unable to bind to the AMPA-R, which may contribute to its lower risk of seizure.

TAK-137 increased proliferation of progenitor cells in the hippocampus over a broader range of doses (0.1–1 mg/kg, p.o. in mice and 0.3–3 mg/kg, p.o. in rats). Moreover, TAK-137 improved cognitive performance of monkeys in the DMTS task over a broader range of doses (0.03–1 mg/kg, p.o.). TAK-137 may have a lower risk of a bell-shaped response than LY451646. Unlike in a previous report, LY451646 did not significantly increase the proliferation of neural progenitor cells in our assays. Effective doses of LY451646 for the enhancement of proliferation of neural progenitor cells or BDNF mRNA expression are reported to change depending on treatment duration [18, 27]. However, despite our attempts to optimize assay conditions, we were unable to observe significant effects of LY451646 on these endpoints.

LY451646 activated AMPA-Rs in the absence of agonist in primary neurons in both the patch-clamp study and the Ca^{2+} influx assay, while it induced Ca^{2+} influx in a glutamate-dependent manner in GluA1i CHO cells. In line with this observation, LY404187, a racemic mixture that includes LY451646, was reported to induce large currents at concentrations higher than 1 μ M during the recording (in the absence of agonist) in a patch-clamp study using primary neurons [28], while LY451646 was reported to show no intrinsic activity in cell lines expressing AMPA-Rs [29, 30]. Thus, LY451646 may have agonistic properties against physiological AMPA-Rs. [3H]-LY395153, of the same chemotype as LY451646, is reported to bind to rat cerebral cortical membranes in the absence of agonist [31]. In the previous study, we found that each AMPA-R potentiator required different concentration of glutamate to activate AMPA-R; OXP1 required lower concentrations of glutamate compared with HBT1 to activate AMPA-R [20]. We speculate that LY451646 may bind to native AMPA-R at channel-closed state under very low concentrations of endogenous glutamate or by insufficient steric interference as with Compound-2, although further studies are needed.

In summary, the present study shows that TAK-137 is a novel AMPA-R potentiator with lower risks of a bell-shaped dose–response and seizures. Since our discovery of TAK-137, we have identified a novel AMPA-R potentiator, TAK-653, using the screening strategy described here. TAK-653 is currently under evaluation in clinical trials.

ACKNOWLEDGEMENTS

We wish to express our sincere thanks to Ayumi Fukakusa for supporting the behavior studies, Aki Hirokawa, and Shigeru Igaki for providing recombinant proteins, Lane Weston and Gyorgy Snell for supporting the X-ray crystallography analysis, Shizu Tsukada for supporting the FACS analysis, Takanobu Kuroita, Masakuni Kori, and Takashi Miki for their guidance and kind suggestions on medicinal chemistry, and Masashi Toyofuku and Eiji Honda for SAR study of TAK-137-related compounds.

ADDITIONAL INFORMATION

Supplementary Information accompanies this paper at (<https://doi.org/10.1038/s41386-018-0213-7>).

Competing interests: The authors are employees of Takeda Pharmaceutical Company Limited. The authors declare no competing interests.

Publisher's note: Springer Nature remains neutral with regard to jurisdictional claims in published maps and institutional affiliations.

REFERENCES

1. Ozawa S, Kamiya H, Tsuzuki K. Glutamate receptors in the mammalian central nervous system. *Prog Neurobiol*. 1998;54(5):581–618.
2. Keinänen K, Wisden W, Sommer B, Werner P, Herb A, Verdoorn TA, et al. A family of AMPA-selective glutamate receptors. *Science*. 1990;249(4968):556–560.
3. Nakanishi N, Shneider NA, Axel R. A family of glutamate receptor genes: evidence for the formation of heteromultimeric receptors with distinct channel properties. *Neuron*. 1990;5(5):569–581.
4. Sommer B, Keinänen K, Verdoorn TA, Wisden W, Burnashev N, Herb A, et al. Flip and flop: a cell-specific functional switch in glutamate-operated channels of the CNS. *Science*. 1990;249(4976):1580–1585.
5. Boulter J, Hollmann M, O'Shea-Greenfield A, Hartley M, Deneris E, Maron C, et al. Molecular cloning and functional expression of glutamate receptor subunit genes. *Science*. 1990;249(4972):1033–1037.
6. Fletcher EJ, Nutt SL, Hoo KH, Elliott CE, Korczak B, McWhinnie EA, et al. Cloning, expression and pharmacological characterization of a human glutamate receptor: hGluR4. *Recept Channels*. 1995;3(1):21–31.
7. Kato AS, Siuda ER, Nisenbaum ES, Brecht DS. AMPA receptor subunit-specific regulation by a distinct family of type II TARPs. *Neuron*. 2008;59(6):986–996.
8. Schoft VK, Schopoff S, Jantsch MF. Regulation of glutamate receptor B pre-mRNA splicing by RNA editing. *Nucleic Acids Res*. 2007;35(11):3723–3732.
9. Tomita S. Regulation of ionotropic glutamate receptors by their auxiliary subunits. *Physiology (Bethesda)*. 2010;25(1):41–49.
10. Derkach VA, Oh MC, Guire ES, Soderling TR. Regulatory mechanisms of AMPA receptors in synaptic plasticity. *Nat Rev Neurosci*. 2007;8(2):101–113.
11. O'Neill MJ, Dix S. AMPA receptor potentiators as cognitive enhancers. *IDrugs*. 2007;10(3):185–192.
12. Shaffer CL, Hurst RS, Scialis RJ, Osgood SM, Bryce DK, Hoffmann WE, et al. Positive allosteric modulation of AMPA receptors from efficacy to toxicity: the interspecies exposure-response continuum of the novel potentiator PF-4778574. *J Pharmacol Exp Ther*. 2013;347(1):212–224.
13. Duman RS, Li N, Liu RJ, Duric V, Aghajanian G. Signaling pathways underlying the rapid antidepressant actions of ketamine. *Neuropharmacology*. 2012;62(1):35–41.
14. Beattie EC, Carroll RC, Yu X, Morishita W, Yasuda H, von Zastrow M, et al. Regulation of AMPA receptor endocytosis by a signaling mechanism shared with LTD. *Nat Neurosci*. 2000;3(12):1291–1300.
15. Yamada KA. Modulating excitatory synaptic neurotransmission: potential treatment for neurological disease? *Neurobiol Dis*. 1998;5(2):67–80.
16. Ehlers MD. Reinsertion or degradation of AMPA receptors determined by activity-dependent endocytic sorting. *Neuron*. 2000;28(2):511–525.
17. Fowler JH, Whalley K, Murray T, O'Neill MJ, McCulloch J. The AMPA receptor potentiator LY404187 increases cerebral glucose utilization and c-fos expression in the rat. *J Cereb Blood Flow Metab*. 2004;24(10):1098–1109.
18. Bai F, Bergeron M, Nelson DL. Chronic AMPA receptor potentiator (LY451646) treatment increases cell proliferation in adult rat hippocampus. *Neuropharmacology*. 2003;44(8):1013–1021.
19. Bernard K, Danover L, Thomas JY, Lebrun C, Munoz C, Cordi A, et al. Drug focus: S18986: a positive allosteric modulator of AMPA-type glutamate receptors pharmacological profile of a novel cognitive enhancer. *CNS Neurosci Ther*. 2010;16(5):e193–212.
20. Kunugi A, Tajima Y, Kuno H, Sogabe S, Kimura H. HBT1, a novel AMPA receptor potentiator with lower agonistic effect, avoided bell-shaped response in vitro BDNF production. *J Pharmacol Exp Ther*. 2018;364(3):377–389.

21. Hayashi Y, Nihonmatsu-Kikuchi N, Yu X, Ishimoto K, Hisanaga SI, Tatebayashi Y. A novel, rapid, quantitative cell-counting method reveals oligodendroglial reduction in the frontopolar cortex in major depressive disorder. *Mol Psychiatry*. 2011;16(12):1155–1158.
22. Shiraishi E, Suzuki K, Harada A, Suzuki N, Kimura H. The phosphodiesterase 10A selective inhibitor TAK-063 improves cognitive functions associated with schizophrenia in rodent models. *J Pharmacol Exp Ther*. 2016;356(3):587–595.
23. Traynelis SF, Wollmuth LP, McBain CJ, Menniti FS, Vance KM, Ogden KK, et al. Glutamate receptor ion channels: structure, regulation, and function. *Pharmacol Rev*. 2010;62(3):405–496.
24. Kaae BH, Harpsoe K, Kastrup JS, Sanz AC, Pickering DS, Metzler B, et al. Structural proof of a dimeric positive modulator bridging two identical AMPA receptor-binding sites. *Chem Biol*. 2007;14(11):1294–1303.
25. Sobolevsky AI, Rosconi MP, Gouaux E. X-ray structure, symmetry and mechanism of an AMPA-subtype glutamate receptor. *Nature*. 2009;462(7274):745–756.
26. Ward SE, Bax BD, Harries M. Challenges for and current status of research into positive modulators of AMPA receptors. *Br J Pharmacol*. 2010;160(2):181–190.
27. Mackowiak M, O'Neill MJ, Hicks CA, Bleakman D, Skolnick P. An AMPA receptor potentiator modulates hippocampal expression of BDNF: an in vivo study. *Neuropharmacology*. 2002;43(1):1–10.
28. Gates M, Ogden A, Bleakman D. Pharmacological effects of AMPA receptor potentiators LY392098 and LY404187 on rat neuronal AMPA receptors in vitro. *Neuropharmacology*. 2001;40(8):984–991.
29. Arai AC, Kessler M, Rogers G, Lynch G. Effects of the potent ampakine CX614 on hippocampal and recombinant AMPA receptors: interactions with cyclothiazide and GYKI 52466. *Mol Pharmacol*. 2000;58(4):802–813.
30. Miu P, Jarvie KR, Radhakrishnan V, Gates MR, Ogden A, Ornstein PL, et al. Novel AMPA receptor potentiators LY392098 and LY404187: effects on recombinant human AMPA receptors in vitro. *Neuropharmacology*. 2001;40(8):976–983.
31. Zarrinmayeh H, Bleakman D, Gates MR, Yu H, Zimmerman DM, Ornstein PL, et al. [³H]N-2-(4-(N-benzamido)phenyl)propyl-2-propanesulfonamide: a novel AMPA receptor potentiator and radioligand. *J Med Chem*. 2001;44(3):302–304.